IEEE Access
Multidisciplinary | Rapid Review | Open Access Journal

Received December 24, 2019, accepted February 2, 2020, date of publication February 7, 2020, date of current version February 18, 2020.

Digital Object Identifier 10.1109/ACCESS.2020.2972271

Evaluation of Temperature Vegetation Dryness Index on Drought Monitoring Over Eurasia

SIQI SHI[1], FENGMEI YAO[1], JIAHUA ZHANG[1,2], AND SHANSHAN YANG[2]

[1]Key Laboratory of Computational Geodynamics, College of Earth and Planetary Sciences, University of Chinese Academy of Sciences, Beijing 100049, China
[2]Key Laboratory of Digital Earth Science, Institute of Remote Sensing and Digital Earth (RADI), Chinese Academy of Sciences (CAS), Beijing 100094, China

Corresponding author: Fengmei Yao (yaofm@ucas.ac.cn)

This work was supported in part by the CAS Strategic Priority Research Program under Grant XDA19030402, in part by the Natural Science Foundation of China under Grant 31671585 and Grant 41871253, in part by the Key Basic Research Project of Shandong Natural Science Foundation of China under Grant ZR2017ZB0422, and in part by the Taishan Scholar Project of Shandong Province under Grant TSXZ201712.

ABSTRACT This study explored the applicability of Temperature Vegetation Dryness Index (TVDI) derived from MODIS (Moderate Resolution Imaging Spectroradiometer) normalized difference vegetation index (NDVI) and land surface temperature (LST) data for drought monitoring in Eurasia from April to September during 2005 - 2014. TVDI was calculated based on the vegetation index/temperature trapezoid eigenspace (VITT) in this study. The Standardized Precipitation Evapotranspiration Index in three time scales (SPEI-01, SPEI-03, SPEI-06) and the Essential Climate Variable surface soil moisture product (ECV-SM) was used to evaluate the performance of TVDI over Eurasia, and to assess the sensitivity of TVDI to different land-cover types. The records of drought events from Emergency Events Database (EM-DAT) were also used to validate TVDI. The results indicated that TVDI negatively responded to SPEIs about 77.43%, 72.01%, and 75.95% of lands respectively, of which 29.84%, 33.93%, and 25.59% were subjected significant relationships ($p<0.05$). A negative correlation between TVDI and SPEIs was detected in most land-cover types, except for evergreen broadleaf forest and deciduous needleaf forest. Similarly, TVDI was also negative correlated with ECV-SM. About 66% of the study areas show negative correlation and 33% of them were statistically significant. There is a highly negative correlation between TVDI and ECV-SM in most types of land cover. Moreover, TVDI could not reflect drought condition correctly when TVDI < 0.40; it could only reflect long-time excessive drought condition when TVDI > 0.86. A comparison of TVDI with drought records demonstrated that the TVDI could capture drought events in study area.

INDEX TERMS Continental scales, drought monitoring, land-cover types, Eurasia, temperature vegetation dryness index.

I. INTRODUCTION

Drought is a complex natural phenomenon that caused by the imbalance of precipitation and evapotranspiration [1], [2]. It usually occurs with a lack of precipitation and results in a decrease of soil moisture content, even affects plant growth when it last a long time [3]. More importantly, the intensity and frequency of drought is becoming more serious on the background of global warming [4]. Therefore, drought monitoring is vital for prevention and mitigation of disasters, and avoiding and reducing the loss of agricultural economy [5].

The associate editor coordinating the review of this manuscript and approving it for publication was Jon Atli Benediktsson.

In recent decades, many indexes, such as Palmer Drought Severity Index (PDSI) [6], Standardized Precipitation Index (SPI) [7], and Standardized Precipitation Evapotranspiration Index (SPEI) [8] have been proposed and widely used to monitor drought. Many studies have validated PDSI is an good drought index for drought monitoring conditions in different regions [9], [10], whereas its time scale is relatively single. The SPI and SPEI can be achieved for flexible time scales. SPI captures the decisive factor—precipitation in the formation of drought, but it ignored the effects of temperature on drought. SPEI combined the simplicity of calculation, multi-temporal nature of SPI, and the sensitivity to evapotranspiration of PDSI. Many studies have used

SPEI to analyze spatial and temporal characteristic of drought in many regions [10], [11]. In recent years, remote sensing data with wider spatial coverage is gradually applied to derive drought indexes in monitoring spatiotemporal pattern of drought. A important finding is that the normalized difference vegetation index (NDVI) [12] can be used to reflect vegetation drought conditions [13], [14]. According to the definition of NDVI, a number of vegetation indexes were developed in detecting drought, such as Vegetation Condition Index (VCI) [15], [16], Enhanced Vegetation Index (EVI) [17]. However, vegetation index is closely related to the greenness of vegetation and is often referred to as a greenness index rather than a drought index [18]. The land surface temperature (LST) is sensitive to crown water content and soil moisture content, while land-cover types could severely affect the relationship between LST and soil moisture content [19]. It means that only using LST data is not applicable for drought monitor when the study area has various land-cover types. For example, the crop water stress index (CWSI) [20], [21], was applicable to only full vegetation areas [24].

However, there are some studies which show that integrating NDVI and LSI can offer more complete information on drought with requires from bare soil to complete vegetation coverage [22], and scientists established many indices by combining satellite data of LST and NDVI [19], [23], [24]. One of them is the temperature vegetation dryness index (TVDI), which is based on the empirical parameterization of feature space established by the relationship between vegetation index and land surface temperature [25]. A lot of studies have used TVDI for drought monitoring, crop yields estimating and soil moisture estimating for different small scales. Son *et al.* [19] showed that TVDI from MODIS (Moderate Resolution Imaging Spectroradiometer) Terra products of monthly NDVI and 8-day LST could reflect drought in the Lower Mekong Basin. Holzman *et al.* [22] estimated soil moisture and the relationship with crop yield using MODIS AQUA 8-day LST and 16-day NDVI in agro-climatic zones of Argentine Pampas. In spite of the triangle method could be used to monitoring drought or estimating soil moisture, the LST-NDVI feature space model is affected by many factors, such as spatial domain size changes [26], vegetation cover [27] and so on. These factors might cause uncertainties of the LST-NDVI feature space, including the unstable dry/wet edges, which couldn't clearly express the theoretical edge of space [28]. In the TVDI calculation model, the wet and dry edge equations play a very important role. However, studies about LST-NDVI feature space for continental spatial domain size, the comparison of TVDI with other indexes, and the evaluation of TVDI was less. Moreover, there was few research studies on the sensitivity of TVDI to different land-cover types.

In Eurasia, there are abundant agricultural resources with high added value of agricultural in Eurasia region, however, the ecosystem is complex and diverse, and the ecological environment in part of Eurasia is fragile, it has

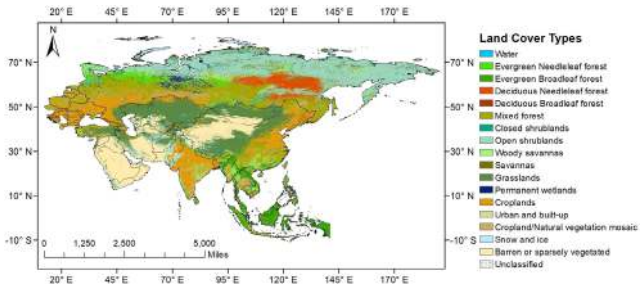

FIGURE 1. Land cover classification map generated by the MODIS International Geosphere-Biosphere Program (IGBP) of 2012.

a profound impact on regional development [29]. Moreover, global warming made frequent disasters with increased drought, which brings serious stress to the fragile ecologic environment [30].

The objectives of this study was 1) to analyze the LST-NDVI feature space and calculate TVDI over Eurasia, 2) evaluate the application of TVDI using SPEIs (SPEI-01, SPEI-03, SPEI-06) and Essential Climate Variable surface soil moisture product (ECV-SM) at continental scale and land cover scale. 3) validate TVDI on drought monitoring with drought events from Emergency Events Database (EM-DAT).

II. STUDY AREA AND DATA

A. STUDY AREA

The study area is the Eurasian continent, which covers a total area of about 50 million km^2. The Eurasian continent stretches from 10°52'S to 79°59'N, and from 179°58'W to 179°58'E. With such a large area, it comprises many climatic zones and complex natural environments [31], [32]. According to Köppen-Geiger climate classification [33], it covers equatorial climates, arid climates, warm temperature climates, snow climates, and polar climates. Moreover, the land-cover types in the region are abundant, primarily in forests (evergreen, deciduous), grasslands, croplands, and barren/sparsely vegetated (Figure 1), with an area of 32.2 million km^2, 21.7 million km^2, 13.9 million km^2, and 22.3 million km^2. The forests occupied the largest area. And there are more than more than 60% of the total areas occupied by arid and semi-arid grasslands, deserts and fragile high-altitude ecological areas, which are characterized by dry climate and low rainfall [29]. Overall, the ecological environment is fragile, and drought events occur frequently. The overall ecological environment is fragile, and drought events occur frequently [29]. Fig.1 showed the types of land cover in the study area developed by using the International Geosphere-Biosphere Program (IGBP) global vegetation classification scheme of MODIS land-cover types product (MCD12Q1, 2012).

B. DATA

1) MODIS DATA

Monthly NDVI and 8-day LST data with 1km spatial resolution from MODIS are used in this study, which are

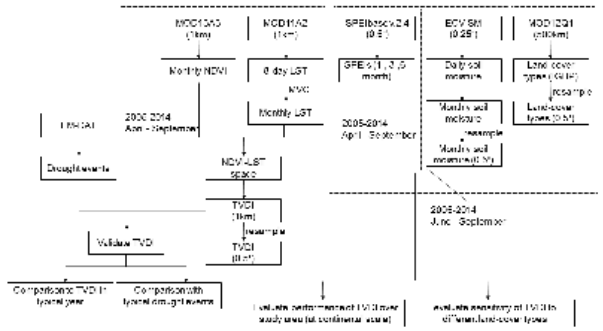

FIGURE 2. The flowchart for this study.

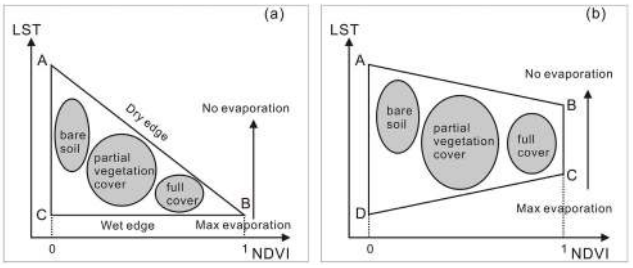

FIGURE 3. A conceptual LST-NDVI triangle (a, modified from Sandholt *et al.* [25]) and a conceptual LST-NDVI trapezoid (b, modified from Yan *et al.* [39]).

obtained from National Aeronautics and Space Administrations (NASA) (https://ladsweb.modaps.eosdis.nasa.gov) for 2005-2014. Months from April to September every year was selected in this study. For 8-day LST, data with staring Julian days 97 through 273 was used. These two data were used to calculate TVDI. The MODIS land-cover type product (MCD12Q1, 2012) with IGBP global vegetation classification scheme was used to define the land cover classification over Eurasia.

2) SPEI AND ECV-SM DATA

Global SPEI dataset (SPEI v2.4) with time scales at 1-, 3-, and 6-months and 0.5° spatial resolution were obtained from http://digital.csic.es/handle/10261/128892 [38]. Furthermore, the daily ECV-SM with 0.25° resolution, developed with the support of the European Space Agency Climate Change Initiative (ESA CCI, https://www.esa-soilmoisture-cci.org/node/230) was also used in this study for evaluating the performance of TVDI on drought monitoring. This remote sensing data contains the ACTIVE, PASSIVE, and the COMBINED product. The active soil moisture data was applied to regions with moderate vegetation density, and passive soil moisture data was applied to arid or semi-arid regions [34]. The combined product was blended together by the ''Active Product'' and the ''Passive Product'', which can better reflect the soil moisture of various land-cover types. In consideration of diverse land-cover types over the study area, the ''Combined Product'' as NetCDF-4-classic file format covering from 2005 to 2014 was used. It was available at http://esa-sst-cci.org.

3) DROUGHT RECORDS DATA

The EM-DAT which was established by the World Health Organization (WHO) and the Belgian Government was a source used to evaluate ability of TVDI to monitor drought. This database provided records and effects of droughts around the world from 1900 to the present day (https://www.emdat.be).

III. METHODOLOGY

Figure 2 showed the flowchart for this study. Monthly TVDI was calculated by monthly LST and monthly NDVI data. For monthly LST, it was calculated by taking Maximum Value Composite (MVC) with the 8-day LST data for DOY97-273 after masking the fill and missing values. Then we build NDVI-LST feature space for every month of April to September for each year. Finally, according to these feature space, monthly TVDI was produced. Here, we gave an example of the calculated of monthly LST-NDVI scatterplots in the first part of result section.

Firstly, the quality of monthly ECV-SM data was checked, and monthly data with incomplete images was removed from the analysis. Monthly ECV-SM data from Months (June - September) with complete data during 2005 - 2014 was used in this analysis at last. To analyze TVDI with SPEIs and ECV-SM at annual scale, we averaged monthly TVDI from April to September, monthly SPEIs from April to September and monthly ECV-SM from June to September to obtain the annual TVDI, annual SPEIs and annual ECV-SM, respectively. To match the resolution of SPEIs, TVDI, ECV-SM data, and land-cover types product were both spatially resampled to 0.5° by bilinear interpolation methods. SPEIs and ECV-SM were used to evaluate the performance of TVDI over Eurasia at large scales. With the aid of MOD12Q1, the sensitivity of TVDI to different land-cover types was evaluated. Lastly, drought events from EM-DAT was used to validate the ability of TVDI for monitoring drought.

A. TEMPERATURE VEGETATION DRYNESS INDEX

Carlson *et al.* [23] and Price [35] found the scatter diagram of NDVI and LST would present a trapezoid, as shown in Figure 3a. Later, based on the model of the LST-NDVI triangle, Sandholt *et al.* [25] proposed TVDI, and he regarded wet edge as a parallel line. In addition, Moran *et al.* [36] defined the vegetation index/temperature trapezoid (VITT) based on the relationship between temperature and vegetation. This trapezoidal model has also been used to calculate the TVDI index in many studies [26], [37]–[39]. In combination with the actual scatter plot, the wet edge is not considered as a parallel line. We use a linear fit to fit the wet edge. For the study area, with various land-cover types, TVDI can be applied to drought monitoring well, because the principle of TVDI requires that sufficiently large study area, the surface coverage ranges from bare soil to complete vegetation coverage, and soil moisture changes Drought becomes humid [22].

TABLE 1. Drought categories For TVDI [41].

	TVDI
Normal	0-0.67
Slight	0.67-0.74
Moderate	0.74-0.80
Severe	0.80-0.86
Excessive	0.86-1.00

[a]We define long-term excessive drought as a state in which TVDI > 0.86 for more than three months; short-term excessive drought as a state in which TVDI > 0.86 for not more than three months.

TVDI could be constructed through the relationship between NDVI and LST as Figure 3b.

TVDI could be calculated using following equations:

$$\mathrm{TVDI} = \frac{LST - LST_{min}}{LST_{max} - LST_{min}} \tag{1}$$

where LST is the land surface temperature of any pixel, LST_{min} is the lower horizontal line of the triangle/trapezoid, defining the wet edge; LST_{max} is the maximum surface temperature, defining the dry edge:

$$LST_{min} = a_1 + b_1 * \mathrm{NDVI} \tag{2}$$

$$LST_{max} = a2 + b2 * \mathrm{NDVI} \tag{3}$$

Equation (2) is called wet edge equation, and (3) is called dry edge equation, both of them are determined by linear regression analysis. a1, b1, and a2, b2 are coefficients of wet edge equation and dry edge equation respectively. Pixels (NDVI $<$ 0 and LST $<$ 200 K) were excluded from analysis for that they might represent inland water bodies [40]. Applying the least-squares regression fitting to extract the maximum LST value and the minimum LST value of the NDVI interval in step of 0.01 from the LST-NDVI trapezoid to obtain the fitting equations for the dry edge and the wet edge. TVDI values variable from 0 to 1, the closer to 1, the closer to dry edge, which means more drought. The values of TVDI were classified into five intensity categories (Table 1).

B. VERIFICATION OF RESULTS

1) CONTINENTAL SCALE

Pearson's correlation coefficient (R) was used to analyze comparison between monthly TVDI and monthly SPEIs, monthly ECV-SM in the spatial pattern. To further discuss the linkages of annual TVDI with annual SPEIs and annual ECV-SM, the scatterplots of TVDI with SPEIs and ECV-SM for 2012 were established with a TVDI interval of 0.01. The annual TVDI, annual SPEIs and annual ECV-SM were averaged by monthly TVDI from April to September, monthly SPEIs from April to September and monthly ECV-SM from June to September, respectively. These scatterplots exhibited the different relationships of TVDI with SPEIs and ECV-SM over different TVDI ranges. Pearson correlation coefficient (R) were used to analyze the relationship between TVDI and SPEI.

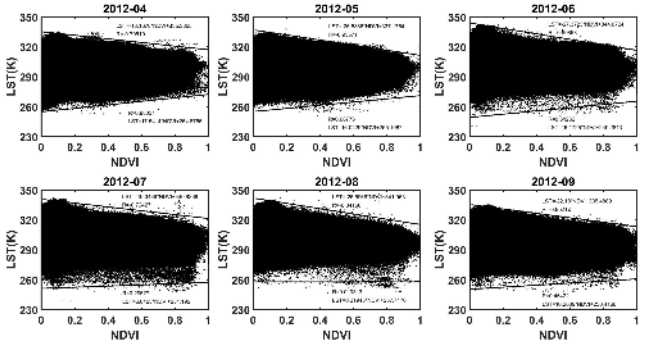

FIGURE 4. LST-NDVI scatterplots in months (April - September) for 2012.

2) LAND COVER SCALE

According to MODIS IGBP classification scheme, the Eurasian continent has 17 land cover types. In this analysis, the areas of water, Permanent wetlands, Urban and built-up, snow and ice, and barren were not considered. In addition, we removed the closed shrub lands and savannas due to scattered distributions and less areas, which might cause mixed-pixel and type-error when resampling land-cover types product from 500m to 0.5° resolution. To explore the performance of TVDI under different land-cover types, TVDI was compared with SPEIs and ECV-SM using the Pearson correlation coefficient (R) under different land-cover types. The distribution and dispersion of R at $p<0.05$ for pixels with different land-cover types were analyzed.

3) DROUGHT RECORDS

To evaluate the capability of TVDI to monitor drought, typical drought year of 2012 and several extreme drought events recorded in EM-DAT as well as literatures over Eurasia in 2005-2014 were analyzed and compared to TVDI. Area weighted average TVDI and SPEI-06 for drought-affected regions were calculated.

IV. RESULTS AND DISCUSSION

A. LST-NDVI SCATTERPLOTS

The LST-NDVI scatterplot is very important for calculating TVDI. We calculated the scatterplots for each month of the year, and only the results for 2012 are shown here (Figure 4). All monthly LST-NDVI scatterplots during the study period were showed in Fig S1. As shown in Figure 4, the range of NDVI is from 0 to 1, indicating that the vegetation coverage in study area ranges from bare to full coverage, which was in line with the TVDI calculation principles. The results show that the LST_{max} has a significant negative correlation with NDVI, and they could be used to build dry edge model. All the slopes of the dry edge in the LST-NDVI feature space were less than 0, indicating that LST_{max} was decreasing with NDVI increasing. The correlation coefficient (R) in each month were in the range from -0.96 to -0.72. Also worth noting was the wet edge, it is generally considered parallel to the horizontal axis, which means that LST_{min} does not

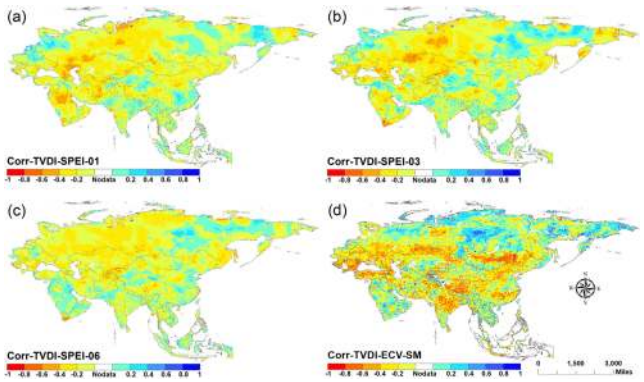

FIGURE 5. Spatial correlation coefficient values between TVDI and SPEI-01 (a), SPEI-03 (b), SPEI-06 (c), ECV-SM (d) for 2005 - 2014 respectively.

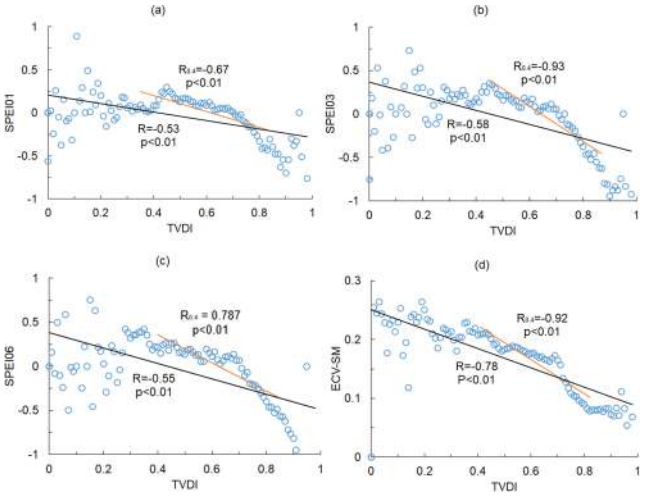

FIGURE 6. The scatterplots and correlation coefficient R and $R_{0.4}$ values between TVDI and SPEI-01 (a), SPEI-03 (b), SPEI-06 (c), ECV-SM (d) for 2012. R was calculated using the values of 0 <TVDI <1, $R_{0.4}$ was calculated using the values of 0.4 <TVDI <0.86.

change with the NDVI. However, the slopes of the wet edge in this study are all greater than 0 (Fig.4, Fig.S1). Thus it is reasonable to linearly fit wet edge instead of considering the wet edge as a line parallel to the horizontal axis.

B. COMPARISON OF INDICES AT CONTINENTAL SCALE

The monthly TVDI was evaluated with monthly SPEIs and ECV-SM through Pearson correlation coefficient. Figure 5 showed the spatial correlation coefficient values between TVDI and SPEI-01, SPEI-03, SPEI-06, and ECV-SM for 2005 – 2014 respectively. The spatial distributions of P-values were showed in Fig. S2. Spatially, TVDI was negatively correlated with SPEIs and ECV-SM. And TVDI showed relatively larger correlation with ECV-SM and SPEI-01 than SPEI03, SPEI06.

As shown in Figure 5a, b, and c, the distribution of R between TVDI and SPEIs displayed similar spatial patterns over the whole study area. TVDI negatively responded to SPEIs about 77.43%, 72.01%, and 75.95% of total areas respectively, and about 29.84%, 33.93%, and 25.59% areas, the correlation coefficients are statistically significant ($p<0.05$). The high correlation values ($R<-0.6$) between TVDI and SPEIs were mainly observed in eastern regions of Europe, western regions of Asia, Balkan Peninsula, and central parts of Russia. These regions are mainly featured with humid temperate climate covered by mixed forests, grassland, and croplands, or arid climate. However, the TVDI had positive correlation with SPEIs in needleleaf forest and evergreen broadleaf forest regions in Russia and southeast Asia, and in humid regions in China. This may be the strong influence of land-cover types and environmental factors. These regions are mainly featured with extremely cold climate or (sub-) tropical humid climate. Vegetation growth in cold region is mainly constrained by temperature and solar radiation. Increased solar radiation under short-term drought conditions could contribute to vegetation growth, which might be a reason for the positive correlation between TVDI and SPEI [42].

Similarly, TVDI was also negative correlated with ECV-SM. About 66.07% of study areas showed negative

TABLE 2. The Statistical Results of Correlation Between TVDI and SPEI-01, SPEI-03, SPEI-06, and SM.

index	R (correlation coefficient)			P-Value	
	<0	>0	mean	<0.05	>0.05
SPEI-01	77.43%	22.57%	-0.25	29.84%	70.16%
SPEI-03	72.01%	27.99%	-0.23	33.93%	66.07%
SPEI-06	75.95%	24.41%	-0.20	25.59%	74.41%
SM	66.07%	33.93%	-0.27	33.17%	66.83%

R values and 33.17% of them were statistically significant ($p<0.05$). The high correlation values ($R<-0.6$) mainly located in mid-latitude and low-latitude regions. TVDI showed positive respond to ECV-SM in a high-latitude region, especially in areas covered by shrub lands and forests (Figure 1), polar region, and Siberian parts of Russia. For polar region and Siberian parts of Russia, due to wide range of frozen soil, the retrieval of soil moisture from satellite acquisitions was unreliable [43]. Overall, TVDI was in good agreement with ECV-SM.

To further investigate the relationship between TVDI and SPEIs, ECV-SM, we used the scatterplots between them to find their relationship. As shown in Figure 6, taking 2012 as an example, the scatterplot between TVDI and SPEI, ECV-SM showed that TVDI are generally negative correlated with SPEIs and ECV-SM. Especially when the values of TVDI in the range of 0.40-0.86, there was a significant strong negative correlation between TVDI and SPEIs. However, when TVDI < 0.40 (the wet) or so, there was almost no specific linear relationship between TVDI and SPEIs, but there was a negative correlation between TVDI and ECV-SM. It illustrated SPEI had great uncertainty in humid areas [44], and it resulted in the anomalous correlation between TVDI

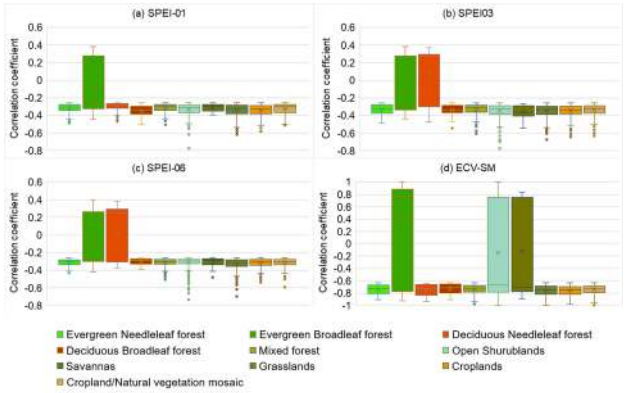

FIGURE 7. The box plots of Correlation coefficients of TVDI and SPEI-01(a), SPEI-02(b), SPEI-03(c), and ECV-SM(d) under different land-cover types during months (April - September) of 2005-2014 (at $p<0.05$). The color zone in this figure references to Figure 1.

and SPEIs in humid regions in spatially in Figure 5a, b, and c. In addition, when the value of TVDI reached a higher level, TVDI > 0.86 or so (the excessive drought), the negative relationship between TVDI and SPEI-01, SPEI-03, and ECV-SM became weakened, especially with SPEI-01. This suggested that TVDI could monitor the long-term excessive drought, however, for short-term excessive drought (<3 month), TVDI cannot reflect its condition and effect. It might be concluded that using TVDI to monitoring drought was suitable for normal, slight, moderate, severe drought and long-time excessive drought.

C. COMPARISON OF INDICES AT LAND COVER SCALE

The correlation between TVDI and SPEIs, ECV-SM at land cover scale was shown in Figure 7. At most land-cover types, the correlation between TVDI and SPEI was negative. But for evergreen broadleaf forest and deciduous needleaf forest, TVDI was positively correlated with SPEIs. The evergreen broadleaf forest was mostly observed in tropical humid climate, such as Southeast Asia. Moist forests in tropics has high resilience during drought [45], [46], as shown by the positive correlation between TVDI and SPEIs. The deciduous needleaf forest are mainly distributed in cold temperate regions, Xu *et al.* [47] showed growth of cold temperate forests may negatively respond to SPEI. In order to be able to observe the correlation between TVDI and SPEIs more clearly, we separately extracted the data under the cover of other vegetation types, which were showed in Figure Fig. S3. The deciduous broadleaf forest showed the most sensitive response to drought at 1-month scale ($R_{spei01\_mean} = -0.36$), while the savannas was least sensitive ($R_{spei01\_mean} = -0.31$). The correlation between TVDI and SPEI-03 was the strongest under open shrublands ($R_{spei01\_mean} = -0.37$), but the weakest under grassland ($R_{spei01\_mean} = -0.33$). TVDI had the strongest correlation with SPEI-06 under open shrublands ($R_{spei01\_mean} = -0.35$), and the weakest correlation under mixed forest ($R_{spei01\_mean} = -0.30$). At the evergreen needleleaf forest, mixed forest, open shrublands, cropland/natural vegetation mosaic, and open shrublands, TVDI were the most sensitive to drought at 3-month timescale, respectively. And deciduous broadleaf forest, grasslands, and croplands showed the most sensitive response to drought at 1-month timescale, respectively.

A highly negative correlation between TVDI and ECV-SM was detected in most types of land cover. However, in the areas covered by evergreen broadleaf forest, open shrublands, and savannas, TVDI and ECV-SM showed a positive correlation in some pixels, especially in evergreen broadleaf forest. Luo *et al.* [48] found the variation in NDVI of evergreen broadleaf forest were very low, and drought might not be a limiting factor for vegetation activity. On the other hand, it could tolerate drought, and it could use water in deep soil to sustain growth [45], [49]. While ECV-SM stands for surface soil moisture [50]. For open shrublands, the third quartile of R was 0.77, while the mean and median of R were −0.44 and −0.66, respectively. It indicated that only a small number of pixels showed a positive correlation between TVDI and ECV-SM. According to Figure 5d, some inaccurate pixels of ECV-SM data from frozen soil regions existed in this statistic. The savannas occupied a small percentage of the whole area (Figure 1), but inter-quartile range was high (R values from −0.77 to 0.75), demonstrating diverse relationships between TVDI and ECV-SM. Savannas located in cold humid zone and tropical humid zone respond differently to surface soil moisture due to rooting habits and water strategies [47]. In addition, regardless of evergreen broadleaf forest, open shrublands, and savannas, TVDI had the strongest negative correlation with ECV-SM in evergreen needleleaf forest ($R_{ECV-SM\_mean} = -0.75$), and had the weak correlation in mix forest ($R_{ECV-SM\_mean} = -0.72$).

D. COMPARISON BETWEEN TVDI AND DROUGHT RECORDS

1) COMPARISON TO TVDI IN TYPICAL YEAR

According to the records from EM-DAT, the number of drought events in 2012 was the highest during 2005-2014 over Eurasia, with 52 drought events (at province scale). The drought events recorded in the EM-DAT during April to September for 2012 of Eurasia were captured by TVDI (Figure 8). For example, in Thailand, there was 12,000,000km^2 affected by drought from April to August in 2012; Ukraine was affected by drought from April to July in 2012; western Russian was affected by drought from June to August in 2012. Although there was no more than one month error appeared between EM-DAT and TVDI, it is notable that EM-DAT was a collection of records created by organizations [51], lacking sufficient objectivity [52]. We also compared droughts of 2012 mentioned in literatures with TVDI results. In South Asia, the areas of moderate and severe drought expended from April to July, and consecutive droughts in Pakistan and India extensively affected crop yield, Gao *et al.* [53]. In East Asia, various

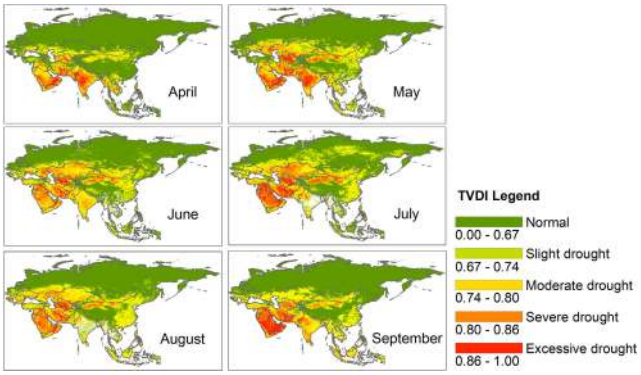

FIGURE 8. TVDI results during April to September for 2012.

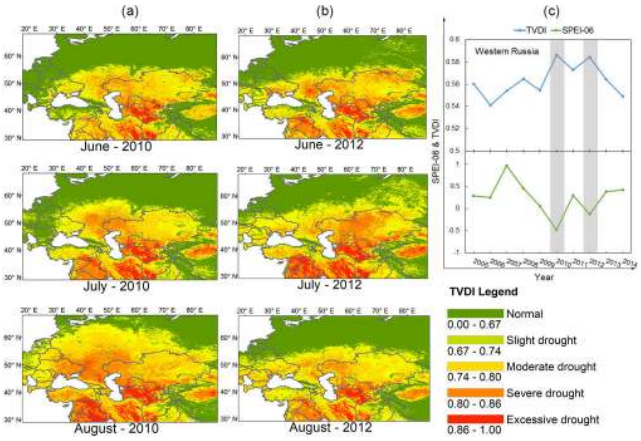

FIGURE 9. Drought occurrence in 2010 (a) and 2012 (b) in western Russia with TVDI. Area weighted average TVDI, SPEI-06 results for western Russia regions for 2005 – 2014 period (c). Vertical gray bars denote years with typical drought events.

intensity of droughts occurred in southwestern China, southern China and Huang-huai area in spring and autumn [54]. These drought events were successfully detected by TVDI.

2) COMPARISON WITH TYPICAL DROUGHT EVENTS IN STUDY AREA

Several regional drought examples from TVDI were highlighted here. In western Russia, food crop yields have fallen by 25-30% and livestock production has severely suffered from the Heat Wave and its associated drought event in 2010 [55]. This drought was clearly recognized by the TVDI results, including Eastern Europe, Georgia, Kazakhstan, and western Russia, especially from June to August, 2010 (Figure 9a, and c). In addition, another major drought event occurred in 2012 was also captured by TVDI and SPEI-06 (Figure 9b, and c). Lupo *et al.* [56] and Spinoni *et al.* [57] suggested that drought in 2010 was heavier than in 2012, and EM-DAT showed affected areas in 2010 with 1,400,000km^2 was larger than 2012 with 1,140,000 km^2, this condition was consistent with TVDI and SPEI-06 results.

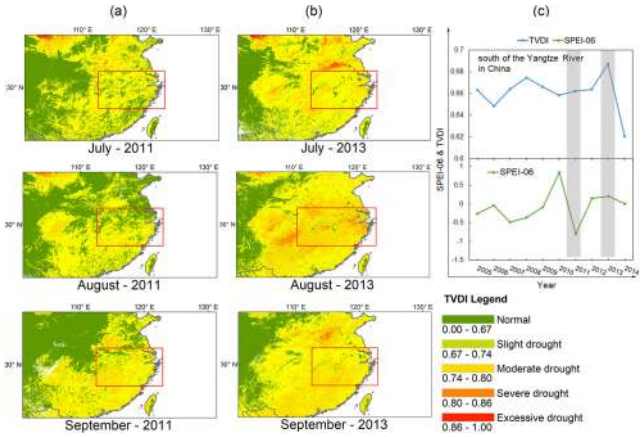

FIGURE 10. Drought occurrence in 2011 (a) and 2013 (b) in the south of Yangtze River with TVDI. The Yangtze River area was shown in red box. Area weighted average TVDI, SPEI-06 results for the Yangtze River for 2005 - 2014 period (c). Vertical gray bars denote years with typical drought events.

Apart from the samples in Europe described above, the other drought occurred in Asia were also analyzed and compared with TVDI. The south of the Yangtze River is dominated by tropical and subtropical monsoon climates, with high-temperature and rainy weather in summer, and low frequency of droughts. However, widespread severe drought due to higher temperature and less rain occurred in 2013. According to the report of China Meteorological Administration (CMA) in 2013, the precipitation in most areas in the Yangtze River was 52.6% less compared to normal years. the drought began to appear in the middle of June,; and developed to the worst in August, thenfaded to moderate in September [58]. The process of drought development was accurately captured by TVDI (Figure 10b). The area weighted average TVDI came to the same conclusion. While it was not detected by SPEI-06. (Figure 10c), which provided the evidence of uncertainty of SPEIbase in the south of Yangtze River. It was notable that SPEI-06 captured drought in 2011, but TVDI failed. The main cause for drought in the south of the Yangtze River of 2011 was the decrease of rainfall, and this drought lasted for less than three month [59]. In the calculation of TVDI, precipitation was not considered as a direct factor, NDVI was considered to be insensitive to short-term precipitation reduction [42], the two factors might cause the limitation of TVDI under short-time reduce rainfall conditions.

V. CONCLUSION

It seems very ambitious and doubtable to monitor large-area drought with a unique index given the diverse climates, environmental features, and land-cover types. This study suggested the potential high performance of TVDI as an index to monitor drought in most regions over Eurasia. Based only on MODIS remote sensing data, TVDI was applied at a large-area scale and long-time scale in this study. It was evaluated with SPEIs and ECV-SM at continental scale and land cover

scale, respectively; and it also was validated with drought records.

We have found that TVDI was significantly negative correlated ($p<0.05$) with SPEIs in humid temperate climate covered by mixed forests, grassland, and croplands, or arid climate, but not in extremely cold climate or (sub-) tropical humid climate. And it also showed that that TVDI was suitable for long-time excessive drought when TVDI>0.86. In the situation of slight, moderate and severe drought with the value of TVDI in the range of 0.40-0.86 or so, it could reflect drought correctly. However, it could not monitor drought correctly when TVDI<0.40. In addition, TVDI was in good agreement with ECV-SM, which means TVDI was suitable for estimating soil moisture over Eurasia.

According to comparison with land-cover types, TVDI was most sensitive to SPEI-01 in deciduous broad-leaved forests, and was most sensitive to both SPEI-03 and SPEI-06 in open shrublands. In most land-cover types, TVDI was sensitive to drought at 3-month timescale. While in deciduous Broadleaf forest, grasslands, and croplands, TVDI was more sensitive to drought at 1-month timescale. Additionally, there was a highly negative correlation between TVDI and ECV-SM in most types of land cover, of which TVDI showed the highest negative correlation in evergreen needleleaf forest. However, due to living environments, rooting habits and water strategies of vegetation, TVDI had positive correlation with SPEIs in evergreen needleleaf forest, and deciduous needleleaf forest; and had positive correlation with ECV-SM in evergreen needleleaf forest, open shrublands, and savannas.

Furthermore, TVDI was in agreement with drought records, but the capability of TVDI to monitor drought is poor in conditions that they only caused by reduced rainfall. It might because TVDI was derived by NDVI and LST, while precipitation was not integrated directly in the calculation of TVDI, and NDVI was considered to be insensitive to short-term precipitation reduction.

In general, our results demonstrated that TVDI could be used to monitor drought and capture drought events over Eurasia. It was suitable for estimating soil moisture, and slight, moderate, severe drought, or long-time excessive drought, but it should not be used to monitor situations of short-time excessive drought and wet.

REFERENCES

[1] D. Etkin, J. Medalye, and K. Higuchi, "Climate warming and natural disaster management: An exploration of the issues," *Climatic Change*, vol. 112, nos. 3–4, pp. 585–599, Jun. 2012.

[2] J. Zhang, Z. Zhou, F. Yao, L. Yang, and C. Hao, "Validating the modified perpendicular drought index in the north China region using *in situ* soil moisture measurement," *IEEE Geosci. Remote Sens. Lett.*, vol. 12, no. 3, pp. 542–546, Mar. 2015.

[3] G. B. Senay, "Drought monitoring and assessment: Remote sensing and modeling approaches for the famine early warning systems network," in *Hydro-Meteorological Hazards, Risks, and Disasters*, J. F. Shroder, P. Paron, and G. D. Baldassarre, Eds. Boston, MA, USA: Elsevier, 2015, ch. 9, pp. 233–262.

[4] R. K. Pachauri, *Contribution of Working Groups I, II and III to the Fifth Assessment Report of the Intergovernmental Panel on Climate Change*. Geneva, Switzerland: IPCC, 2014, p. 151.

[5] Q. Zhang, L. Han, J. Jia, L. Song, and J. Wang, "Management of drought risk under global warming," *Theor. Appl. Climatol.*, vol. 125, nos. 1–2, pp. 187–196, Jul. 2016.

[6] W. C. Palmer, "Keeping track of crop moisture conditions, nationwide: The new crop moisture index," *Weatherwise*, vol. 21, no. 4, pp. 156–161, Aug. 1968.

[7] T. B. McKee, N. J. Doesken, and J. Kleist, "The relationship of drought frequency and duration to time scales," in *Proc. 8th Conf. Appl. Climatol.* Boston, MA, USA: American Meteorological Society, 1993, vol. 17, no. 22, pp. 179–183.

[8] S. M. Vicente-Serrano, S. Beguería, and J. I. López-Moreno, "A multiscalar drought index sensitive to global warming: The standardized precipitation evapotranspiration index," *J. Climate*, vol. 23, no. 7, pp. 1696–1718, Apr. 2010.

[9] Y. Wang, R. Lu, Y. Ma, Y. Sang, H. Meng, and S. Gao, "Annual variation in PDSI since 1897 AD in the Tengger Desert, Inner Mongolia, China, as recorded by tree-ring data," *J. Arid Environ.*, vol. 98, pp. 20–26, Nov. 2013.

[10] H. Yan, S.-Q. Wang, J.-B. Wang, H.-Q. Lu, A.-H. Guo, Z.-C. Zhu, R. B. Myneni, and H. H. Shugart, "Assessing spatiotemporal variation of drought in China and its impact on agriculture during 1982–2011 by using PDSI indices and agriculture drought survey data," *J. Geophys. Res. Atmos.*, vol. 121, no. 5, pp. 2283–2298, Mar. 2016.

[11] X. Li, J. Sha, and Z.-L. Wang, "Comparison of drought indices in the analysis of spatial and temporal changes of climatic drought events in a basin," *Environ. Sci. Pollut. Res.*, vol. 26, no. 11, pp. 10695–10707, 2019.

[12] J. W. Rouse, Jr., R. Haas, J. Schell, and D. Deering, "Monitoring vegetation systems in the Great Plains with ERTS," in *Proc. 3rd Earth Resour. Technol. Satell. (ERTS) Symp.*, 1973.

[13] S. K. Jain, R. Keshri, A. Goswami, A. Sarkar, and A. Chaudhry, "Identification of drought-vulnerable areas using NOAA AVHRR data," *Int. J. Remote Sens.*, vol. 30, no. 10, pp. 2653–2668, 2009.

[14] L. Geng, M. Ma, W. Yu, X. Wang, and S. Jia, "Validation of the MODIS NDVI products in different land-use types using *in situ* measurements in the Heihe river basin," *IEEE Geosci. Remote Sens. Lett.*, vol. 11, no. 9, pp. 1649–1653, Sep. 2014.

[15] F. Kogan, "Application of vegetation index and brightness temperature for drought detection," *Adv. Space Res.*, vol. 15, no. 11, pp. 91–100, Jan. 1995.

[16] F. N. Kogan, "Droughts of the late 1980s in the United States as derived from NOAA polar-orbiting satellite data," *Bull. Amer. Meteor. Soc.*, vol. 76, no. 5, pp. 655–668, May 1995.

[17] A. Huete, K. Didan, T. Miura, E. Rodriguez, X. Gao, and L. Ferreira, "Overview of the radiometric and biophysical performance of the MODIS vegetation indices," *Remote Sens. Environ.*, vol. 83, nos. 1–2, pp. 195–213, Nov. 2002.

[18] T. Jackson, "Vegetation water content mapping using Landsat data derived normalized difference water index for corn and soybeans," *Remote Sens. Environ.*, vol. 92, no. 4, pp. 475–482, Sep. 2004.

[19] N. Son, C. Chen, C. Chen, L. Chang, and V. Minh, "Monitoring agricultural drought in the lower mekong basin using MODIS NDVI and land surface temperature data," *Int. J. Appl. Earth Observ. Geoinf.*, vol. 18, pp. 417–427, Aug. 2012.

[20] S. Idso, R. Jackson, P. Pinter, R. Reginato, and J. Hatfield, "Normalizing the stress-degree-day parameter for environmental variability," *Agricult. Meteorol.*, vol. 24, pp. 45–55, Jan. 1981.

[21] N. Kumar, A. Poddar, V. Shankar, C. S. P. Ojha, and A. J. Adeloye, "Crop water stress index for scheduling irrigation of Indian mustard (Brassica juncea) based on water use efficiency considerations," *J. Agronomy Crop Sci.*, vol. 206, no. 1, pp. 148–159, 2020.

[22] M. Holzman, R. Rivas, and M. Piccolo, "Estimating soil moisture and the relationship with crop yield using surface temperature and vegetation index," *Int. J. Appl. Earth Observ. Geoinf.*, vol. 28, pp. 181–192, May 2014.

[23] T. N. Carlson, E. M. Perry, and T. J. Schmugge, "Remote estimation of soil moisture availability and fractional vegetation cover for agricultural fields," *Agricult. Forest Meteorol.*, vol. 52, nos. 1–2, pp. 45–69, Aug. 1990.

[24] X. Hu, H. Ren, K. Tansey, Y. Zheng, D. Ghent, X. Liu, and L. Yan, "Agricultural drought monitoring using European space agency sentinel 3A land surface temperature and normalized difference vegetation index imageries," *Agricult. Forest Meteorol.*, vol. 279, Dec. 2019, Art. no. 107707.

[25] I. Sandholt, K. Rasmussen, and J. Andersen, "A simple interpretation of the surface temperature/vegetation index space for assessment of surface moisture status," *Remote Sens. Environ.*, vol. 79, nos. 2–3, pp. 213–224, Feb. 2002.

[26] J. Tian, H. Su, X. Sun, S. Chen, H. He, and L. Zhao, "Impact of the spatial domain size on the performance of the Ts-VI triangle method in terrestrial evapotranspiration estimation," *Remote Sens.*, vol. 5, no. 4, pp. 1998–2013, Apr. 2013.
[27] X. Cao, Y. Feng, and J. Wang, "An improvement of the Ts-NDVI space drought monitoring method and its applications in the Mongolian plateau with MODIS, 2000-2012," *Arabian J. Geosci.*, vol. 9, no. 6, p. 433, May 2016.
[28] Y. Liu and H. Yue, "The temperature vegetation dryness index (TVDI) based on bi-parabolic NDVI-Ts space and gradient-based structural similarity (GSSIM) for long-term drought assessment across Shaanxi Province, China (2000–2016)," *Remote Sens.*, vol. 10, no. 6, p. 959, Jun. 2018.
[29] Q. Liu, "Ecological environment monitoring for sustainable development goals in the Belt and Road region," *J. Remote Sens.*, vol. 22, no. 4, pp. 686–708, 2018.
[30] A. Dai, "Drought under global warming: A review," *Wiley Interdiscipl. Rev., Climate Change*, vol. 2, no. 1, pp. 45–65, Jan. 2011.
[31] Z. W. Gu and L. Zhang, "Analysis of the characteristics of vegetation changes in eurasia," (in Chinese), *Acta Agric. Univ. Jiangxiensis*, vol. 34, no. 02, pp. 329–333, 2012.
[32] M. Z. Fan and B. Fan, "Shift scenarios of mean centers in vegetation ecosystems in Eurasia," (in Chinese), *Acta Ecol. Sinica*, vol. 39, no. 14, pp. 5028–5039, 2019.
[33] M. Kottek, J. Grieser, C. Beck, B. Rudolf, and F. Rubel, "World map of the Köppen-Geiger climate classification updated," *Meteorologische Zeitschrift*, vol. 15, no. 3, pp. 259–263, Jul. 2006.
[34] D. Chung *et al.* (2014). *ECV Production, Fusion of Soil Moisture Products: Algorithm Theoretical Baseline Document, Version 2*. Accessed: Jan. 15, 2019. [Online]. Available: http://www.esa-soilmoisture-cci.org
[35] J. Price, "Using spatial context in satellite data to infer regional scale evapotranspiration," *IEEE Trans. Geosci. Remote Sens.*, vol. 28, no. 5, pp. 940–948, Sep. 1990.
[36] M. Moran, T. Clarke, Y. Inoue, and A. Vidal, "Estimating crop water deficit using the relation between surface-air temperature and spectral vegetation index," *Remote Sens. Environ.*, vol. 49, no. 3, pp. 246–263, Sep. 1994.
[37] L. Sun, R. Sun, X. Li, S. Liang, and R. Zhang, "Monitoring surface soil moisture status based on remotely sensed surface temperature and vegetation index information," *Agricult. Forest Meteorol.*, vols. 166–167, pp. 175–187, Dec. 2012.
[38] W. Wang, Z.-Z. Zhang, X.-G. Wang, and H.-M. Wang, "Evaluation of using the modified water deficit index derived from MODIS vegetation index and land surface temperature products for monitoring drought," in *Proc. IEEE Int. Geosci. Remote Sens. Symp.*, Jul. 2012, pp. 5951–5954.
[39] H. Yan, G. Zhou, F. Yang, and X. Lu, "DEM correction to the TVDI method on drought monitoring in karst areas," *Int. J. Remote Sens.*, vol. 40, nos. 5–6, pp. 2166–2189, Mar. 2019.
[40] A. Karnieli, N. Agam, R. T. Pinker, M. Anderson, M. L. Imhoff, G. G. Gutman, N. Panov, and A. Goldberg, "Use of NDVI and land surface temperature for drought assessment: Merits and limitations," *J. Climate*, vol. 23, no. 3, pp. 618–633, Feb. 2010.
[41] S. Q. Zhang, Q. T. Qing, M. T. Hou, and J. D. Feng, "Remote sensing and impact estimation for Sichuan hot-drought based on temperature vegetation dryness index," *Trans. CSAE*, no. 09, pp. 141–146+294, 2007.
[42] L. Huang, B. He, L. Han, J. Liu, H. Wang, and Z. Chen, "A global examination of the response of ecosystem water-use efficiency to drought based on MODIS data," *Sci. Total Environ.*, vols. 601–602, pp. 1097–1107, Dec. 2017.
[43] C. Pratola, B. Barrett, A. Gruber, and E. Dwyer, "Quality assessment of the CCI ECV soil moisture product using ENVISAT ASAR wide swath data over Spain, Ireland and Finland," *Remote Sens.*, vol. 7, no. 11, pp. 15388–15423, Nov. 2015.
[44] B. I. Cook, J. E. Smerdon, R. Seager, and S. Coats, "Global warming and 21st century drying," *Climate Dyn.*, vol. 43, nos. 9–10, pp. 2607–2627, Nov. 2014.
[45] B. Sun, H. Zhao, and X. Wang, "Effects of drought on net primary productivity: Roles of temperature, drought intensity, and duration," *Chin. Geogr. Sci.*, vol. 26, no. 2, pp. 270–282, Apr. 2016.
[46] Q. Zhang, L.-Q. Gao, Z.-L. Han, X.-F. Li, L.-H. Wang, and S.-D. Liu, "Effectiveness and safety of endoscopic resection for gastric GISTs: A systematic review," *Minimally Invasive Therapy Allied Technol.*, vol. 27, no. 3, pp. 127–137, May 2018.
[47] H.-J. Xu, X.-P. Wang, C.-Y. Zhao, and X.-M. Yang, "Diverse responses of vegetation growth to meteorological drought across climate zones and land biomes in northern China from 1981 to 2014," *Agricult. Forest Meteorol.*, vol. 262, pp. 1–13, Nov. 2018.
[48] X. Luo, X. Chen, L. Wang, L. Xu, and Y. Tian, "Modeling and predicting spring land surface phenology of the deciduous broadleaf forest in northern China," *Agricult. Forest Meteorol.*, vols. 198–199, pp. 33–41, Nov. 2014.
[49] L. Y. Cao, T. Zhou, H. Luo, Z. Li, P. P. Xu, and X. Liu, "The mediation of forest coverage in the responses of forest to climate drought," (in Chinese), *J. Beijing Normal Univ. (Nature Sci.)*, vol. 55, no. 2, pp. 240–247, 2019.
[50] C. Pratola, B. Barrett, A. Gruber, G. Kiely, and E. Dwyer, "Evaluation of a global soil moisture product from finer spatial resolution SAR data and ground measurements at Irish sites," *Remote Sens.*, vol. 6, no. 9, pp. 8190–8219, Aug. 2014.
[51] D. Guha-Sapir, R. Below, and P. Hoyois. (2016). *EM-DAT: The CRED/OFDA International Disaster Database*. Accessed: Mar. 1, 2019. [Online]. Available: https://www.emdat.be/emdat_db/
[52] N. Sánchez, Á. González-Zamora, J. Martínez-Fernández, M. Piles, and M. Pablos, "Integrated remote sensing approach to global agricultural drought monitoring," *Agricult. Forest Meteorol.*, vol. 259, pp. 141–153, Sep. 2018.
[53] H. Gao, J. H. Zhang, and X. Q. Xia, "Drought monitoring by remote sensing over India and Pakistan based on temperature vegetation dryness index," (in Chinese), *Remote Sens. Inf.*, vol. 31, no. 04, pp. 62–68, 2016.
[54] H. X. Duan, S. P. Wang, and J. Y. Feng, "Chinese drought conditions as well as impact and causes in 2012," (in Chinese), *J. Arid Meteor.*, vol. 31, no. 1, pp. 220–229, 2013.
[55] D. Barriopedro, E. M. Fischer, J. Luterbacher, R. M. Trigo, and R. Garcia-Herrera, "The hot summer of 2010: Redrawing the temperature record map of Europe," *Science*, vol. 332, no. 6026, pp. 220–224, Apr. 2011.
[56] A. R. Lupo, I. I. Mokhov, Y. G. Chendev, M. G. Lebedeva, M. Akperov, and J. A. Hubbart, "Studying summer season drought in western Russia," *Adv. Meteorol.*, vol. 2014, pp. 1–9, Feb. 2014.
[57] J. Spinoni, G. Naumann, J. V. Vogt, and P. Barbosa, "The biggest drought events in Europe from 1950 to 2012," *J. Hydrol., Regional Stud.*, vol. 3, pp. 509–524, Mar. 2015.
[58] H. X. Duan, S. P. Wang, and J. Y. Feng, "Chinese drought conditions as well as effects and causes in summer of 2013," (in Chinese), *J. Arid Meteor.*, vol. 31, no. 3, pp. 633–640, 2013.
[59] H. X. Duan, S. P. Wang, and J. Y. Feng, "Chinese drought conditions as well as impact and causes in 2011," (in Chinese), *J. Arid Meteor.*, vol. 30, no. 1, pp. 136–147, 2012.

SIQI SHI received the B.S. degree in geographic information science from Jiangxi Normal University (JXNU), China, in 2017. She is currently pursuing the M.S. degree with the University of Chinese Academy of Sciences (UCAS), Beijing, China. Her research interests include drought monitoring and assessment and remote sensing application.

FENGMEI YAO received the Ph.D. degree in meteorology from the Institute of Atmospheric Physics, Chinese Academy of Sciences (CAS), Beijing, China, in 2005. Since August 2005, she has been an Assistant Professor with the Graduated University of Chinese Academy of Sciences. Since 2017, she has been a Full Professor with the College of Earth and Planetary Sciences, University of Chinese Academy of Sciences. She has published more than 100 peer-reviewed articles, 20 international conferences papers, and four books. She has been involved in climate change and effect on vegetation and agriculture, atmospheric environment, and disaster.

JIAHUA ZHANG received the Ph.D. degree in cartography and remote sensing from the Institute of Remote Sensing Applications, Chinese Academy of Sciences (CAS), in 1998. From 1999 to 2001, he held a postdoctoral position with the National Institute for Environmental Studies, Japan. Since 2002, he has been a Professor at the Chinese Academy of Meteorological Sciences. Since 2012, he has also been a Full Professor at the Institute of Remote Sensing and Digital Earth, CAS. His research interests include global climate change and disaster remote sensing, atmospheric environment, land use, and vegetation dynamic. He has published more than 150 peer review articles, 30 international conferences papers, and six books.

SHANSHAN YANG received the B.S. and M.S. degrees from the School of Geography and Remote Sensing, Nanjing University of Information Science and Technology, in 2012 and 2015, respectively. She is currently pursuing the Ph.D. degree with the Institute of Remote Sensing and Digital Earth, Chinese Academy of Sciences, Beijing, China. Her research interests include terrestrial ecosystem water use efficiency, carbon and water cycle, and ecosystem response to climate change.